

UC Santa Barbara

UC Santa Barbara Previously Published Works

Title

Ligand-Mediated C-Br Oxidative Addition to Cycloplatinated(II) Complexes and Benzyl-Me C-C Bond Reductive Elimination from a Cycloplatinated(IV) Complex

Permalink

<https://escholarship.org/uc/item/9fk513hx>

Journal

ACS Omega, 5(44)

ISSN

2470-1343

Authors

Bavi, Marzieh
Nabavizadeh, S Masoud
Hosseini, Fatemeh Niroomand
et al.

Publication Date

2020-11-10

DOI

10.1021/acsomega.0c03573

Peer reviewed

Ligand-Mediated C–Br Oxidative Addition to Cycloplatinated(II) Complexes and Benzyl-Me C–C Bond Reductive Elimination from a Cycloplatinated(IV) Complex

Marzieh Bavi, S. Masoud Nabavizadeh,* Fatemeh Niroomand Hosseini, Fatemeh Niknam, Peyman Hamidizadeh, S. Jafar Hoseini, Fatemeh Raouf, and Mahdi M. Abu-Omar*



Cite This: *ACS Omega* 2020, 5, 28621–28631



Read Online

ACCESS |



Metrics & More

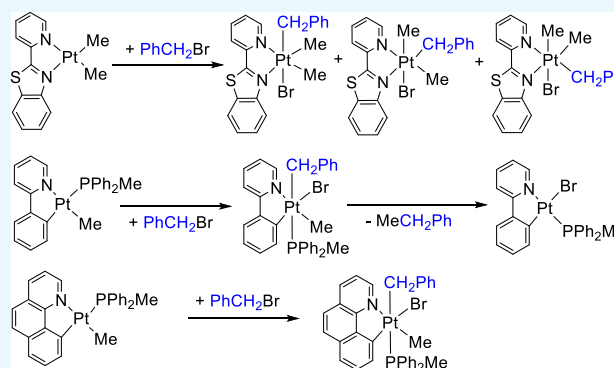


Article Recommendations



Supporting Information

ABSTRACT: Reaction of the Pt(II) complexes [PtMe₂(pbt)], **1a**, (pbt = 2-(2-pyridyl)benzothiazole) and [PtMe(C[^]N)(PPh₂Me)] [C[^]N = deprotonated 2-phenylpyridine (ppy), **1b**, or deprotonated benzo[h]quinoline (bhq), **1c**] with benzyl bromide, PhCH₂Br, is studied. The reaction of **1a** with PhCH₂Br gave the Pt(IV) product complex [PtBr(CH₂Ph)Me₂(pbt)]. The major trans isomer is formed in a trans oxidative addition (**2a**), while the minor cis products (**2a'** and **2a''**) resulted from an isomerization process. A solution of Pt(II) complex **1a** in the presence of benzyl bromide in toluene at 70 °C after 7 days gradually gave the dibromo Pt(IV) complex [Pt(Br)₂Me₂(pbt)], **4a**, as determined by NMR spectroscopy and single-crystal XRD. The reaction of complexes **1b** and **1c** with PhCH₂Br gave the Pt(IV) complexes [PtMeBr(CH₂Ph)(C[^]N)(PPh₂Me)] (C[^]N = ppy; **2b**; C[^]N = bhq, **2c**), in which the phosphine and benzyl ligands are trans. Multinuclear NMR spectroscopy ruled out other isomers. Attempts to grow crystals of the cycloplatinated(IV) complex **2b** yielded a previously reported Pt(II) complex [PtBr(ppy)(PPh₂Me)], **3b**, presumably from reductive elimination of ethylbenzene. UV–vis spectroscopy was used to study the kinetics of reaction of Pt(II) complexes **1a–1c** with benzyl bromide. The data are consistent with a second-order S_N2 mechanism and the first order in both the Pt complex and PhCH₂Br. The rate of reaction decreases along the series **1a** >> **1c** > **1b**. Density functional theory calculations were carried out to support experimental findings and understand the formation of isomers.



INTRODUCTION

There is a great current interest in the chemistry of cyclometalated organometallic compounds on the basis of their applications in stoichiometric and catalytic organic synthesis,^{1–6} optoelectronic devices,^{7–9} therapeutic agents,^{10–12} chemical sensors,¹³ and luminescent probes for biomolecules because of their photophysical properties.^{14–16} Investigations of the cycloplatinated compounds have given rise to many interesting complexes and new mechanistic insights into their reactions.^{17–20} Cyclometalation proceeds by the reaction of Pt(II) precursor complexes, [Pt(aryl)₂(SMe₂)₂] or [PtMe₂(μ-SMe₂)₂], with ligands such as 2-phenylpyridine or benzo[h]quinoline.^{17,21–28}

The C–halide bonds, along with other C–X bonds with large electronegativity differences, are considered as polar substrates in the oxidative addition reactions.^{29,30} Among distinct mechanisms suggested for C–X bond activation, the S_N2 mechanism is quite common. Because oxidative addition reactions are key steps in many catalytic reactions, they are extensively investigated.^{17,31–35} Although the kinetics and mechanism of organic halide addition to organoplatinum(II)

complexes of the general formula [PtR₂(NN)] (R = Me or aryl and NN = 2,2′-bipyridine or 1,10-phenanthroline) are well established,^{30,34,36,37} related reactions with cycloplatinated(II) complexes have been less studied.^{29,38–40}

C–C bond-forming reductive elimination is well recognized as the last step in many catalytic cycles used in organic synthesis.^{41–44} Such processes have been studied extensively including Pt(IV) complexes.^{45–49} Although there are some reports on C–C bond formation from the organoplatinum(IV) complex involving Me–Me or acyl–Me,^{34,46,50–53} a limited number of studies on the intramolecular C–C reductive elimination from Pt(IV) complexes, especially C–C benzyl-methyl reductive elimination, are reported.⁵² Gold-

Received: July 27, 2020

Accepted: September 1, 2020

Published: October 29, 2020



berg and Crumpton reported C–C reductive elimination reactions from Pt(IV) complexes.⁵⁴ Also, we have recently reported on homocoupling of benzene.⁶

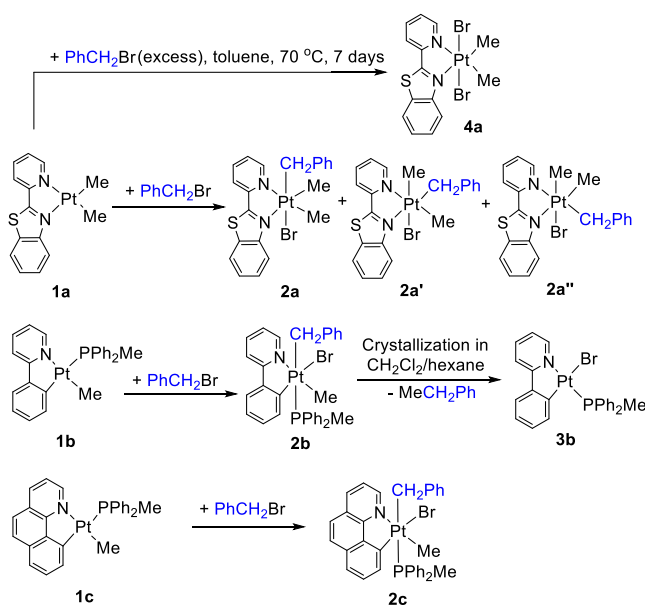
Because our interests lie in the reactivity of cycloplatinated complexes, here, we show that although the cycloplatinated(II) complex [PtMe(C[^]N)(PPh₂Me)] (C[^]N = deprotonated 2-phenylpyridine (ppy), **1b**, or deprotonated benzo[h]-quinoline (bhq), **1c**) reacts with benzyl bromide, PhCH₂Br, to give exclusively the trans addition product, the previously reported complex [PtMe₂(pbt)],⁵⁵ **1a**, (pbt = 2-(2-pyridyl)-benzothiazole) reacts uniquely with PhCH₂Br to give a mixture of isomeric products. The reactivity of Pt(II) centers in these complexes as a nucleophile toward PhCH₂Br is compared. Our kinetic and mechanistic study suggests that the reactions proceed through a bimolecular S_N2 pathway. The resulting cycloplatinated(IV) complex [PtMeBr(CH₂Ph)(ppy)-(PPh₂Me)] undergoes a benzyl-Me C–C bond-forming reductive elimination to give the cycloplatinated(II) complex [PtBr(ppy)(PPh₂Me)]. The experimental findings are also computationally investigated, and the optimized structures of the possible transition states and intermediates were determined.

RESULTS AND DISCUSSION

Synthesis and Characterization of the Complexes.

The routes to prepare the new organoplatinum(IV) complexes are described in Scheme 1.

Scheme 1. C–Br Oxidative Addition and C–C Bond Formation Reductive Elimination at Platinum Complexes



The reaction of a solution of [PtMe(C[^]N)(PPh₂Me)] (**1b**; C[^]N = ppy, **1c**; C[^]N = bhq) with benzyl bromide at room temperature gave the complexes [PtMeBr(CH₂Ph)(C[^]N)-(PPh₂Me)] (**2b**; C[^]N = ppy, **2c**; C[^]N = bhq) in good yields through oxidative addition of PhCH₂Br. Both complexes were characterized using multinuclear ¹H, ³¹P, and ¹³C NMR spectroscopy (see Table 1) and elemental analysis. The characteristic signal in the ¹H NMR spectrum of [PtMeBr(CH₂Ph)(ppy)(PPh₂Me)], **2b** (see Figure 1), is the methylene protons of the benzylplatinum group, which are diastereotopic

and appeared as two doublets of doublets at $\delta = 2.77$ and 3.88 ppm. In the ¹³C NMR spectrum of **2b**, the signal for the C atom of the Me group in PPh₂Me as a doublet appeared in a low field at $\delta = 11.2$ with ¹J(PtC) and ²J(PtC) values of 29 and 16 Hz, respectively, indicating that they are located trans to the C atom of the benzyl group. A doublet with Pt satellites at $\delta = 31.6$ was assigned to the C atom of CH₂ in the benzyl group, which was further confirmed by DEPT ¹³C NMR analysis (see Figure 1). The coupling constants mentioned above are typical values for Pt(IV) complexes.^{44,56–60}


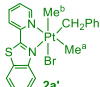

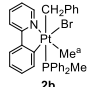
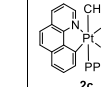
Attempts to grow suitable crystals of the Pt(IV) complex [PtMeBr(CH₂Ph)(ppy)(PPh₂Me)], **2b**, for a single-crystal X-ray diffraction experiment in solvents such as acetone and benzene were not successful. During the crystallization process in CH₂Cl₂/hexane at room temperature, a benzyl-Me C–C bond reductive elimination from cycloplatinated(IV) complex **2b** occurred to give the complex [PtBr(PPh₂Me)(ppy)], **3b**, whose structure was confirmed by single-crystal analysis. It should be mentioned that **3b** had been prepared by direct reaction of the Pt(II) complex [Pt(ppy)(PPh₂Me)-(CF₃COO)] with NaBr.⁵² The suggested mechanism for this process is depicted in Scheme 2.^{50,52,61,62}

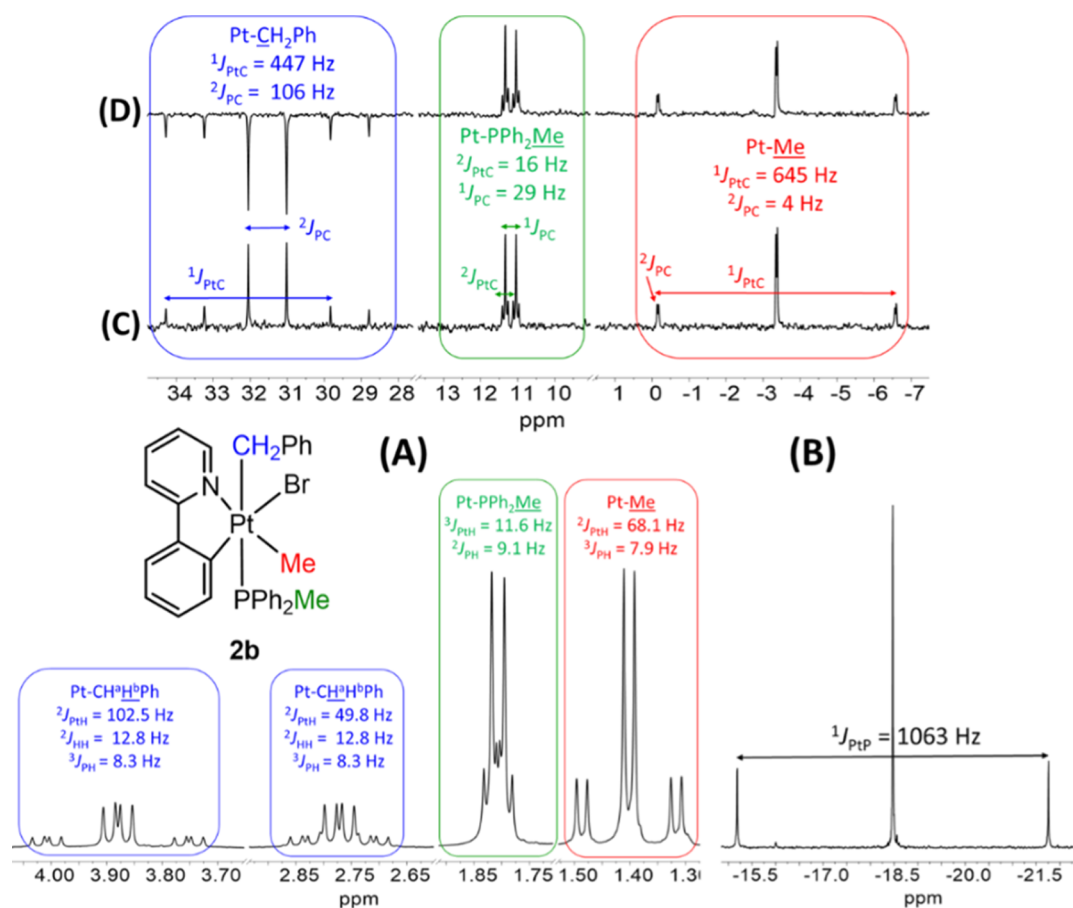
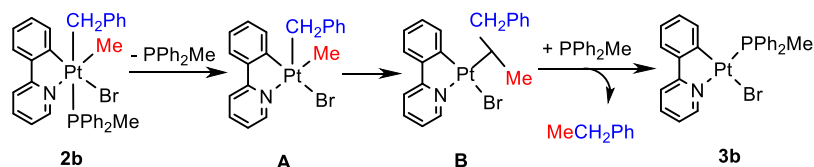
In the reaction of **1a** with PhCH₂Br, the product [PtBr(CH₂Ph)Me₂(pbt)] was shown to be a mixture containing all three possible isomers, **2a** (PhCH₂ being trans to Br), **2a'** (the PhCH₂ ligand being trans to the N ligating atom of the benzothiazole group), and **2a''** (the PhCH₂ ligand being trans to the N ligating atom of the pyridyl group). When the reaction was performed for 2 h, the ratio of the three isomers **2a**/**2a'**/**2a''** was found to be equal to 77:17:6, while after 24 h, the ratio changed to 90:10:0, indicating that the isomers **2a'** (significantly) and **2a''** (completely) returned back to isomer **2a**, being both the kinetic and thermodynamic products. Our density functional theory (DFT) calculations (see the Theoretical Investigation of the Suggested Mechanisms section) are consistent with these experimental results. The trend of stability follows **2a** > **2a'** > **2a''**.

In the ¹H NMR spectrum of the isomer mixture of [PtBr(CH₂Ph)Me₂(pbt)] (see Table 1 and Figure 2), the major isomer **2a** displays two doublets at $\delta = 2.90$ and 3.11 ppm for the PtCH₂ diastereotopic protons, as observed for similar compounds.^{37,60} For the minor isomer **2a'**, the two singlet signals at $\delta = 1.71$ and 1.98 are assigned to the two different methyl ligands being trans to Br and N of the pyridyl ligand, respectively. The isomer **2a'** shows two doublets for diastereotopic protons of the methylene group at $\delta = 2.87$ and 3.10. In the ¹H NMR of isomer **2a''**, two singlets at $\delta = 1.65$ and 1.93 are assigned to the Me ligands trans to Br and N of the benzothiazole ligand, respectively.

In the ¹³C NMR spectrum (see Table 1 and Figure 3), for **2a**, two singlets with Pt satellites are observed for the two different methyl groups directly connected to Pt, trans to N of pyridyl and benzothiazole rings.⁵⁵ The ¹J(PtC) values (see Table 1) are smaller than the corresponding values reported for the methyl groups of complex **1a** (¹J(PtC) = 807 Hz and 844 Hz),⁵⁵ confirming the oxidation of Pt(II) to Pt(IV) by benzyl bromide. The CH₂ of benzyl appears at $\delta = 22.8$ and was confirmed by DEPT ¹³C analysis.⁶³ **2a'** also shows the two singlet resonances for two different methyl ligands being trans to N of the pyridyl ligand and Br. Similar to **2a**, the isomer **2a'** displays a singlet C atom of CH₂, which was confirmed by DEPT ¹³C NMR experiments. The resonances for isomer **2a''** were not resolved in the ¹³C NMR spectrum.

Table 1. NMR Data (Chemical Shifts in ppm and *J* in Hz) for Pt(IV) Complexes

					
Me ^a	$\delta_{\text{H}}, {}^2J_{\text{PtH}}, {}^3J_{\text{PH}}$ 1.78, 76.0	$\delta_{\text{H}}, {}^2J_{\text{PtH}}, {}^3J_{\text{PH}}$ 1.98, 72.2	$\delta_{\text{H}}, {}^2J_{\text{PtH}}, {}^3J_{\text{PH}}$ 1.65, 72.4	$\delta_{\text{H}}, {}^2J_{\text{PtH}}, {}^3J_{\text{PH}}$ 1.36, 68.1, 7.9	$\delta_{\text{H}}, {}^2J_{\text{PtH}}, {}^3J_{\text{PH}}$ 1.59, 68.6, 7.7
	$\delta_{\text{C}}, {}^1J_{\text{PtC}}, {}^2J_{\text{PC}}$ -6.4, 680	$\delta_{\text{C}}, {}^1J_{\text{PtC}}, {}^2J_{\text{PC}}$ -5.8, 718	$\delta_{\text{C}}, {}^1J_{\text{PtC}}, {}^2J_{\text{PC}}$ n.r. ^a	$\delta_{\text{C}}, {}^1J_{\text{PtC}}, {}^2J_{\text{PC}}$ -3.4, 645, 4	$\delta_{\text{C}}, {}^1J_{\text{PtC}}, {}^2J_{\text{PC}}$ ---
Me ^b	$\delta_{\text{H}}, {}^2J_{\text{PtH}}$ 2.05, 76.1	$\delta_{\text{H}}, {}^2J_{\text{PtH}}$ 1.71, 72.0	$\delta_{\text{H}}, {}^2J_{\text{PtH}}$ 1.93, 74.0	---	---
	$\delta_{\text{C}}, J_{\text{PtC}}$ -0.2, 712	$\delta_{\text{C}}, J_{\text{PtC}}$ -0.2, n.r. ^a	$\delta_{\text{C}}, J_{\text{PtC}}$ n.r. ^a	---	---
CH ₂ Ph	$\delta_{\text{H}}^{\text{a}}, {}^2J_{\text{PtH}}^{\text{a}}, {}^3J_{\text{PH}}^{\text{a}}$ 2.90, 85.0	$\delta_{\text{H}}^{\text{a}}, {}^2J_{\text{PtH}}^{\text{a}}, {}^3J_{\text{PH}}^{\text{a}}$ 2.87, 85.2	$\delta_{\text{H}}^{\text{a}}, {}^2J_{\text{PtH}}^{\text{a}}, {}^3J_{\text{PH}}^{\text{a}}$ n.r. ^a	$\delta_{\text{H}}^{\text{a}}, {}^2J_{\text{PtH}}^{\text{a}}, {}^3J_{\text{PH}}^{\text{a}}$ 2.77, 49.8, 8.3	$\delta_{\text{H}}^{\text{a}}, {}^2J_{\text{PtH}}^{\text{a}}, {}^3J_{\text{PH}}^{\text{a}}$ 2.74, 51.4, 9.3
	$\delta_{\text{H}}^{\text{b}}, {}^2J_{\text{PtH}}^{\text{b}}, {}^3J_{\text{PH}}^{\text{b}}$ 3.11, 96.3	$\delta_{\text{H}}^{\text{b}}, {}^2J_{\text{PtH}}^{\text{b}}, {}^3J_{\text{PH}}^{\text{b}}$ 3.10, 97.3	$\delta_{\text{H}}^{\text{b}}, {}^2J_{\text{PtH}}^{\text{b}}, {}^3J_{\text{PH}}^{\text{b}}$ n.r. ^a	$\delta_{\text{H}}^{\text{b}}, {}^2J_{\text{PtH}}^{\text{b}}, {}^3J_{\text{PH}}^{\text{b}}$ 3.88, 102.5, 8.3	$\delta_{\text{H}}^{\text{b}}, {}^2J_{\text{PtH}}^{\text{b}}, {}^3J_{\text{PH}}^{\text{b}}$ 3.92, 101.2, 9.3
	$\delta_{\text{C}}, {}^1J_{\text{PtC}}, {}^2J_{\text{PC}}$ 22.8, 639	$\delta_{\text{C}}, {}^1J_{\text{PtC}}, {}^2J_{\text{PC}}$ 18.6, 648	$\delta_{\text{C}}, {}^1J_{\text{PtC}}, {}^2J_{\text{PC}}$ n.r. ^a	$\delta_{\text{C}}, {}^1J_{\text{PtC}}, {}^2J_{\text{PC}}$ 31.6, 447, 106	$\delta_{\text{C}}, {}^1J_{\text{PtC}}, {}^2J_{\text{PC}}$ ---
PPh ₂ Me	$\delta_{\text{H}}, {}^3J_{\text{PtH}}, {}^2J_{\text{PH}}$ ---	$\delta_{\text{H}}, {}^3J_{\text{PtH}}, {}^2J_{\text{PH}}$ ---	$\delta_{\text{H}}, {}^3J_{\text{PtH}}, {}^2J_{\text{PH}}$ ---	$\delta_{\text{H}}, {}^3J_{\text{PtH}}, {}^2J_{\text{PH}}$ 1.81, 11.6, 9.1	$\delta_{\text{H}}, {}^3J_{\text{PtH}}, {}^2J_{\text{PH}}$ 1.70, 11.8, 9.2
	$\delta_{\text{C}}, {}^2J_{\text{PtC}}, {}^1J_{\text{PC}}$ ---	$\delta_{\text{C}}, {}^2J_{\text{PtC}}, {}^1J_{\text{PC}}$ ---	$\delta_{\text{C}}, {}^2J_{\text{PtC}}, {}^1J_{\text{PC}}$ ---	$\delta_{\text{C}}, {}^2J_{\text{PtC}}, {}^1J_{\text{PC}}$ 11.2, 16, 29	$\delta_{\text{C}}, {}^2J_{\text{PtC}}, {}^1J_{\text{PC}}$ ---
	$\delta_{\text{P}}, {}^1J_{\text{PtP}}$ ---	$\delta_{\text{P}}, {}^1J_{\text{PtP}}$ ---	$\delta_{\text{P}}, {}^1J_{\text{PtP}}$ ---	$\delta_{\text{P}}, {}^1J_{\text{PtP}}$ -18.5, 1063	$\delta_{\text{P}}, {}^1J_{\text{PtP}}$ -18.0, 1064

^an.r. = Not resolved.Figure 1. (A) ¹H (aliphatic region), (B) ³¹P, (C) ¹³C (aliphatic region), and (D) DEPT ¹³C (aliphatic region) NMR spectra of complex **2b** in CDCl₃.Scheme 2. Suggested Mechanism for Benzyl-Me C–C Bond Reductive Elimination from **2b**

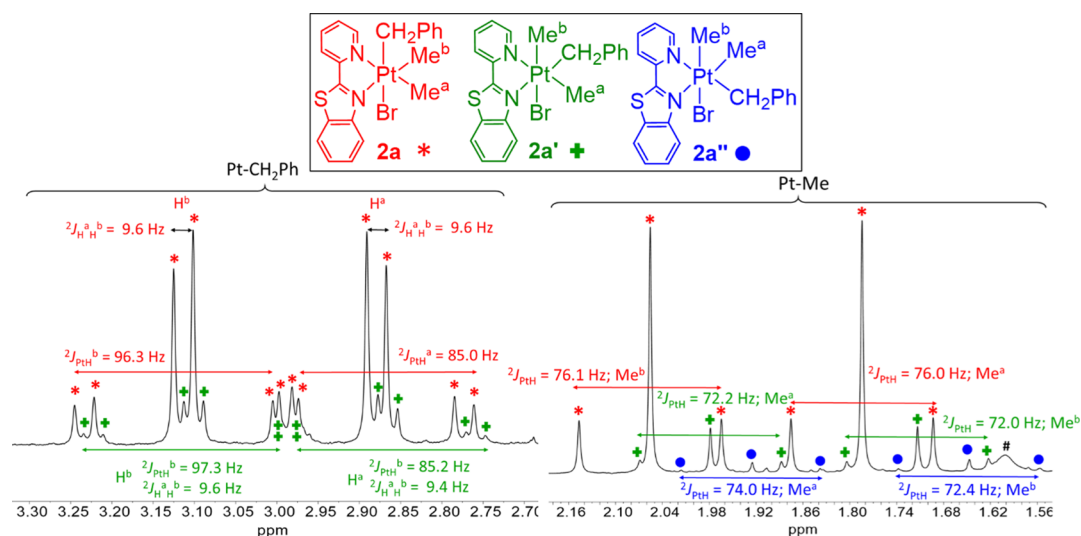


Figure 2. (A) ^1H (aliphatic region) NMR spectrum of the complex $[\text{PtBr}(\text{CH}_2\text{Ph})\text{Me}_2(\text{pbt})]$ in CDCl_3 . The peak labeled # is due to water of the CDCl_3 solvent. The signals for the methylene group of isomer 2a'' were overlapped by those for isomers 2a and 2a' and not resolved.

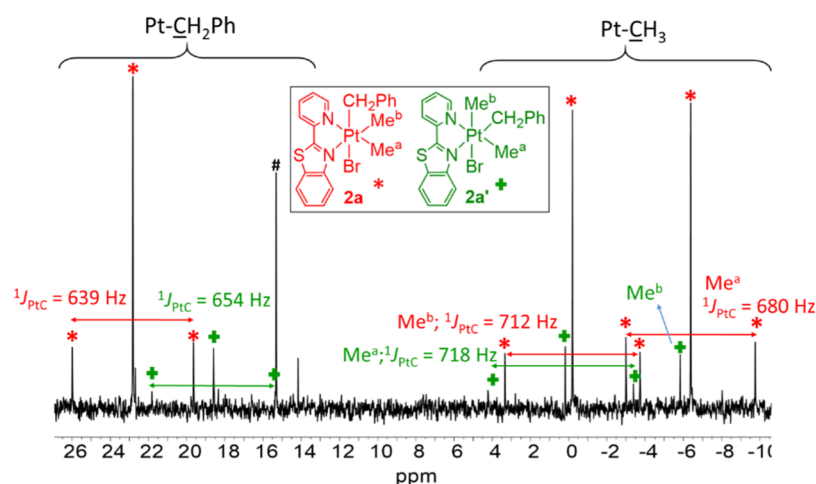


Figure 3. Selected aliphatic regions of the ^{13}C NMR spectrum of $[\text{PtBr}(\text{CH}_2\text{Ph})\text{Me}_2(\text{pbt})]$ in CDCl_3 . Assignments are given on the spectrum. The resonances for isomer 2a'' were not resolved. The peak labeled # is due to the diethyl ether solvent used for purification.

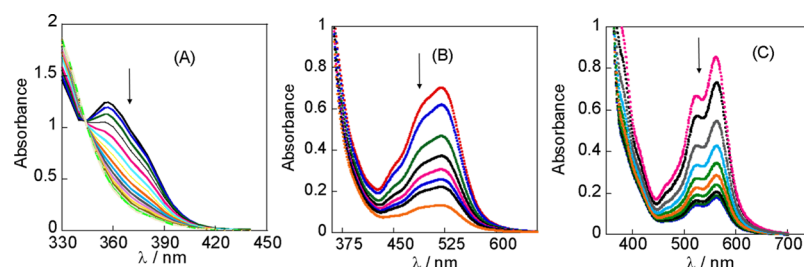


Figure 4. Changes in the UV–visible spectrum during the reaction of $[\text{PtMe}(\text{PPh}_2\text{Me})(\text{ppy})]$, **1b**, ($3 \times 10^{-4} \text{ M}$) with PhCH_2Br in acetone (A) and $[\text{PtMe}_2(\text{pbt})]$, **1a**, ($3 \times 10^{-4} \text{ M}$) with PhCH_2Br in acetone (B) and in toluene (C) at 25°C .

It should be noted that the reaction of complex **1a** with excess of benzyl bromide in toluene at 70°C for 6 days gave the dibromoplatinum(IV) complex $[\text{Pt}(\text{Br})_2\text{Me}_2(\text{pbt})]$, **4a**. Its ^1H NMR spectrum and X-ray crystal structure (Figure S1) are reported in the Supporting Information.

Kinetic Study. The kinetic study of oxidative addition reactions of Pt(II) complexes **1a–c** with PhCH_2Br (and in one case with MeI in order to study the effect of alkyl halide on the rate of reaction) was carried out in acetone (and toluene to

investigate the solvent effect). The rate of the oxidative addition reactions was studied by dissolving complexes **1a–c** in the selected solvent followed by rapid mixing with a known excess of PhCH_2Br . Typical examples of the observed spectral changes and kinetic traces (Abs–time curves) are shown in Figures 4 and 5, respectively. The kinetic traces recorded for these reactions displayed excellent fits to eq 1 (for the pseudo-first-order condition) or eq 2 (for the 1:1 stoichiometric condition).

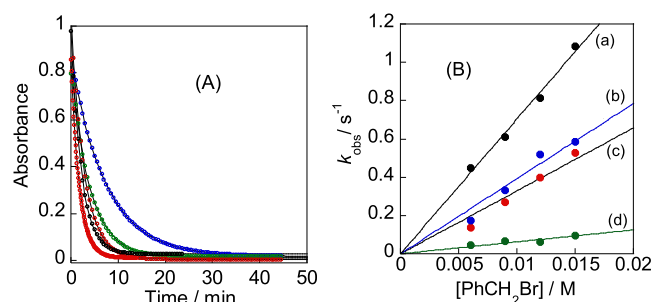


Figure 5. (A) Abs–time curves for the reaction of $[\text{PtMe}_2(\text{pbt})]$, **1a**, (3×10^{-4} M) with PhCH_2Br (0.006–0.015 M, concentration increases reading downward) in toluene at 25 °C. (B) Plots of first-order rate constants ($k_{\text{obs}}/\text{s}^{-1}$) versus concentration of benzyl bromide for the reaction of (a) $[\text{PtMe}_2(\text{pbt})]$, **1a**, with PhCH_2Br in toluene; (b) $[\text{PtMe}(\text{PPh}_2\text{Me})(\text{ppy})]$, **1b**, with MeI in acetone; (c) $[\text{PtMe}(\text{PPh}_2\text{Me})(\text{ppy})]$, **1b**, with PhCH_2Br in acetone; and (d) $[\text{PtMe}(\text{PPh}_2\text{Me})(\text{bhq})]$, **1c**, with PhCH_2Br in acetone at $T = 40$ °C.

The activation parameters (enthalpy and entropy of activation) were obtained from the temperature dependence of k_2 by applying Eyring plots (see Figure 6), and the kinetic

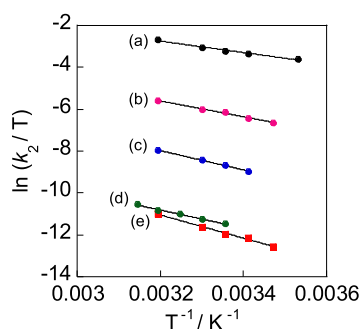


Figure 6. Eyring plots for the reactions of (a) $[\text{PtMe}_2(\text{pbt})]$, **1a**, with PhCH_2Br , in acetone; (b) $[\text{PtMe}_2(\text{pbt})]$, **1a**, with PhCH_2Br , in toluene; (c) $[\text{PtMe}(\text{PPh}_2\text{Me})(\text{ppy})]$, **1b**, with MeI in acetone; (d) $[\text{PtMe}(\text{PPh}_2\text{Me})(\text{bhq})]$, **1c**, with PhCH_2Br in acetone; and (e) $[\text{PtMe}(\text{PPh}_2\text{Me})(\text{ppy})]$, **1b**, with PhCH_2Br in acetone.

data are collected in Table 2. The large negative values of entropy of activation for the reactions studied in the present work are typical of oxidative addition by a common $\text{S}_{\text{N}}2$ mechanism^{29,30,64,65} which involves nucleophilic attack of the Pt center at the methylene group of PhCH_2Br and the formation of a five-coordinate cationic intermediate (see the next section).

The order of the reaction rates of PhCH_2Br with Pt(II) complexes in acetone is **1a** \gg **1c** > **1b**. The slightly observed

increase in rate on going from $[\text{PtMe}(\text{PPh}_2\text{Me})(\text{ppy})]$, **1b**, to $[\text{PtMe}(\text{PPh}_2\text{Me})(\text{bhq})]$, **1c**, by a factor of about 1.5 is probably due to more electron releasing character of the bhq ligand as compared to that of the ppy ligand, which makes the Pt(II) center in **1c** more electron rich than the Pt(II) center in **1b**, toward oxidative addition reactions. The same behavior has been reported for the reactions of H_2O_2 ,⁶⁶ $\text{PhI}(\text{OAc})_2$,⁴⁵ and MeI ⁶⁷ with complexes **1b** and **1c**. The rate of reaction of dimethylplatinum(II) complex **1a** with PhCH_2Br was considerably higher than those obtained for complexes **1b** and **1c**. For example, at 25 °C, the values of k_2 are 11.95 and $0.31 \times 10^{-2} \text{ L mol}^{-1} \text{ s}^{-1}$, respectively, for complexes **1a** and **1b**. Thus, 3 orders of magnitude difference ($10^3\times$) can be attributed to the presence of an extra methyl group (a very strong σ -donor) in **1a** versus an electron-withdrawing phosphine ligand in **1b** and **1c**.

As shown in Table 2, the rates of reaction of complex **1a** in toluene were some 18–20 times slower than those in acetone. We found that probably because the intermediate is ionic, as expected in the classical $\text{S}_{\text{N}}2$ mechanism, reactions are sensitive to the solvent polarity, and consequently, the reactions are faster in acetone than toluene.

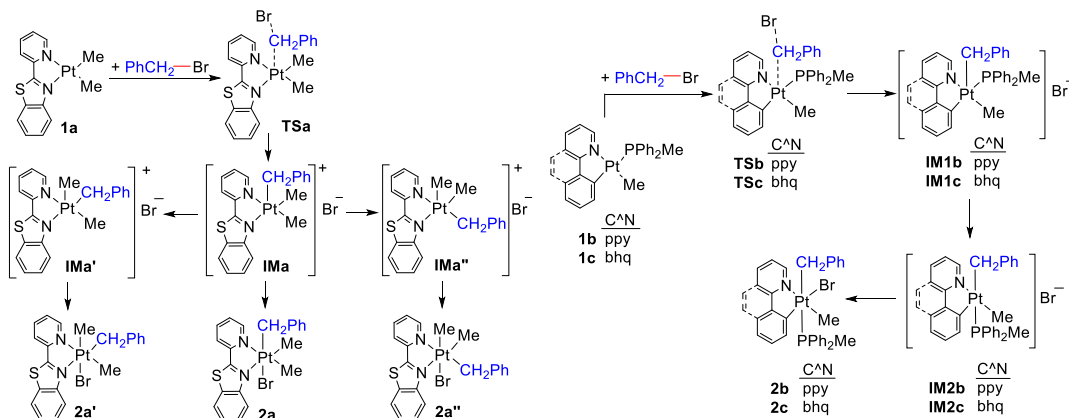
The rates of reaction of complex **1b** with MeI in acetone are faster than those with PhCH_2Br . Two factors can explain this observation. First, the halogen effect in which the rate of the reactions decreases in the order $\text{I} > \text{Br}$ (generally ascribed to “iodide being a better leaving group than bromide”).⁶⁸ Second, the effect of the R group. In $\text{S}_{\text{N}}2$ reactions, the rate of reaction is dependent on the steric of the R group. The bulkier R group (in this instant, benzyl vs Me) has a slower reaction rate.⁶⁹ With due attention to the R group and the halogen effect, the Pt(II) complex **1b** must react faster with MeI as compared to PhCH_2Br . Also, given that these reactions follow second-order kinetics with remarkable reproducibility and the fact that radical scavengers did not affect the rate would rule out the possibility of any radical mechanism.^{30,70} Thus, the above-mentioned observations strongly suggest an $\text{S}_{\text{N}}2$ mechanism of oxidative addition of the benzyl bromide to Pt(II) complexes **1a**–**1c**. Also, the large negative entropies of activation are typical values for oxidative addition by the $\text{S}_{\text{N}}2$ mechanism (see Table 2). It should be noted that PhCH_2Br at 25 °C reacted nearly 1.3 times slower with the unsymmetric benzothiazol complex **1a** ($k_2 = 11.95 \text{ L mol}^{-1} \text{ s}^{-1}$) than the symmetric 2,2'-bipyridine (bpy) derivative, $[\text{PtMe}_2(\text{bpy})]$ ³⁷ ($k_2 = 15.60 \text{ L mol}^{-1} \text{ s}^{-1}$). The same mechanism for the reaction of benzyl bromide with $[\text{PtMe}_2(\text{bpy})]$ has been suggested and supported by the kinetic isotope effect.³⁷

Theoretical Investigation of the Suggested Mechanisms. To get more insight into the suggested mechanism and perform a reliable molecular modeling of the new Pt complexes

Table 2. Second-Order Rate Constants^a and Activation Parameters for the Reactions of $[\text{PtMe}_2(\text{pbt})]$, **1a**, $[\text{PtMe}(\text{PPh}_2\text{Me})(\text{ppy})]$, **1b**, and $[\text{PtMe}(\text{PPh}_2\text{Me})(\text{bhq})]$, **1c**, with PhCH_2Br in Acetone

complex	$\lambda_{\text{max}}/\text{nm}$	$k_2/\text{L mol}^{-1} \text{ s}^{-1}$ at different temperatures					$\Delta H^\ddagger/\text{kJ mol}^{-1}$	$\Delta S^\ddagger/\text{J K mol}^{-1}$
		10 °C	20 °C	25 °C	30 °C	40 °C		
1a ^b	520, (562)	7.66, (0.38)	10.44, (0.47)	11.95, (0.63)	14.29, (0.75)	21.47, (1.17)	22.5 \pm 1.7, (31.5 \pm 1.1)	−148 \pm 6, (−143 \pm 4)
		10 ² $k_2/\text{L mol}^{-1} \text{ s}^{-1}$ at different temperatures						
1b ^c	358	0.10	0.15, [3.75]	0.20, [5.05]	0.31, [6.55]	0.51, [11.00]	45.9 \pm 2.0, [38.2 \pm 0.4]	−142 \pm 7, [−141 \pm 2]
		0.51 ^d	0.83 ^e	0.31	0.39	0.61		
1c	390	0.51 ^d	0.83 ^e	0.31	0.39	0.61	35.8 \pm 1.7	−172 \pm 6

^aEstimated errors in k_2 values are $\pm 5\%$. ^bValues in parenthesis are for toluene. ^cValues in brackets are for MeI . ^dAt 35 °C. ^eAt 45 °C.

Scheme 3. Suggested Mechanisms for Oxidative Addition of Complexes 1a–1c with PhCH₂Br

containing the pbt ligand, a suitable DFT method should be used. DFT calculations have proven to be useful methods for calculations of structures of transition-metal complexes.^{71–73} Among methods and basis sets used for metal complexes, the B3LYP/6-31G(d) level (LANL2DZ potential for Pt) is shown to be a good candidate between accuracy and CPU time of calculations,^{74–76} and therefore, they have been used for mechanistic study and structural optimizations of the Pt complexes.^{45,77,78} The reactions studied in the present work, shown in Scheme 1, have been considered with an emphasis on the differences between the Pt complexes (**1a**, **1b**, and **1c**), alkyl halides (MeI and PhCH₂Br), and the reaction medium, solvent. The suggested mechanism is presented in Scheme 3.

The reaction of PhCH₂Br with the Pt(II) complex **1a** in acetone is initiated by nucleophilic attack^{37,69,79} by the 5d_{z²} HOMO of **1a** on the σ* LUMO of benzyl bromide (Figure 7)

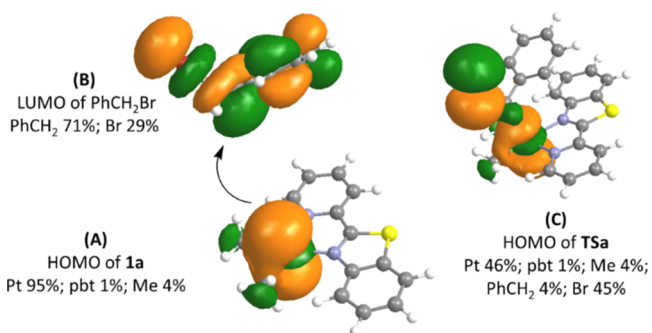


Figure 7. Initiation of S_N2 oxidative addition by interaction of HOMO of **1a** (A) and LUMO of PhCH₂Br (B) to form **TSa** (C). The main compositions (%) of the relevant frontier orbitals of species are also shown. The calculations were performed at the B3LYP/6-31G(d)-LANL2DZ level. See Figure S2 for qualitative frontier molecular orbitals for **1a**, **TSa**, and **2a**.

to give transition state **TSa**. The most significant changes in bond distances of **TSa** are computed for the Br–CH₂ and Pt–CH₂ bonds. The computed bond length of 2.108 Å for Br–CH₂Ph increases to 2.589 Å in **TSa**, while the Pt–CH₂ distance decreases from far apart in the reactants to 2.788 Å. The formation of **TSa** is followed by completely breaking the Br–CH₂ bond and forming the Pt–CH₂ bond, to give intermediate **IMa**, which can abstract bromide to form the isomer **2a** or undergo pseudorotation to give **IMa'** and **IMa''**. The coordination of bromide to these intermediates can then

give isomers **2a'** and **2a''** with an octahedral geometry. As expected, the bond lengths of the starting cycloplatinated(II) complex **1a** are shorter than those of the corresponding Pt(IV) complex **2a**. For example, the Pt–N_{py} and Pt–N_{bz} bonds in **1a** are shorter (2.200 and 2.250 Å, respectively) than those in **2a** (with the values of 2.280 and 2.308 Å, respectively). The energy barrier for the formation of **TSa** in acetone is calculated by DFT to be 23.8 kJ mol^{−1} (see Figure 8), which is in excellent agreement with the experimental value of 22.5 kJ mol^{−1} (see Table 2). The oxidative addition of similar Pt(II) complexes had been also performed using DFT calculations by us and others.^{33,34,38,66,80–82} For example, the computed energy barrier for oxidative addition of [PtMe₂(bpy)] with benzyl bromide was found to be 23.0 kJ mol^{−1},⁶⁹ which is lower than the calculated value of **1a**. This is in agreement with experimental finding where the rate of the reaction of benzyl bromide with **1a** is lower than that for [PtMe₂(bpy)].

There are, in principle, seven possible isomers for the complex [PtBr(CH₂Ph)Me₂(pbt)]. We can quickly delete four of the possible isomers, that is, those having two C atoms in trans positions to one another, because we would have seen only one resonance at the same chemical shift for the two Pt–Me groups (when they are in trans arrangement) or two resonances for the two Pt–Me groups with very different coupling constants (one trans to the PhCH₂ group and another one cis because of different trans influences of C and other atoms) in the ¹H NMR, whereas only two signals with close ²J(PtH) values (see Figure 2) are observed. A series of DFT calculations was performed on the remaining three isomers, **2a**, **2a'**, and **2a''**, depicted in Figure 8 with their relative energies. The enthalpy values obtained from the calculations show the order **2a** < **2a'** < **2a''** with the lowest lying isomer being that the larger PhCH₂ group is located in the axial position as compared with the equatorial position in **2a'** and **2a''** isomers. This agrees with NMR experimental findings where the product ratio of **2a**/**2a'**/**2a''** is 77:17:6.

The reaction of **1a** with PhCH₂Br was also computationally investigated in toluene with lower polarity compared to acetone to understand the effect of the solvent on the energy barrier of oxidative addition reaction. The calculated enthalpy of activation in toluene is 40.5 kJ mol^{−1} (in good agreement with the experimental value of 45.9 kJ mol^{−1}). This solvent effect once again is consistent with an S_N2 mechanism.

It was experimentally found that complex **1b** reacts with MeI faster than benzyl bromide (see Table 2). As shown in Figure 9, the computational investigations show that the ΔH[‡] for the

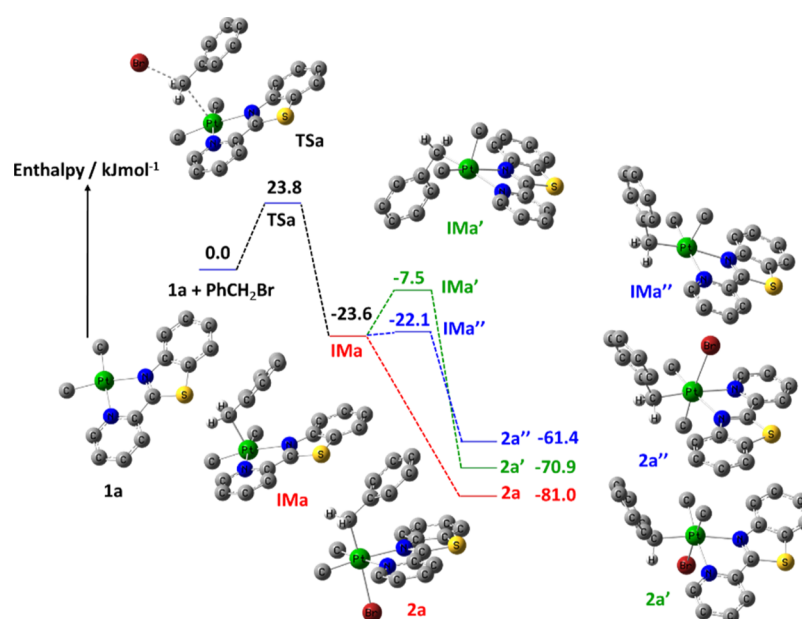


Figure 8. Enthalpy profile for oxidative addition of **1a** with PhCH₂Br in acetone at the B3LYP/6-31G(d)-LANL2DZ level. The optimized structures of the species involved in the reactions are shown. The summation of the energies of the **1a** and PhCH₂Br was considered to be zero, and the other energy levels vary relative to this.

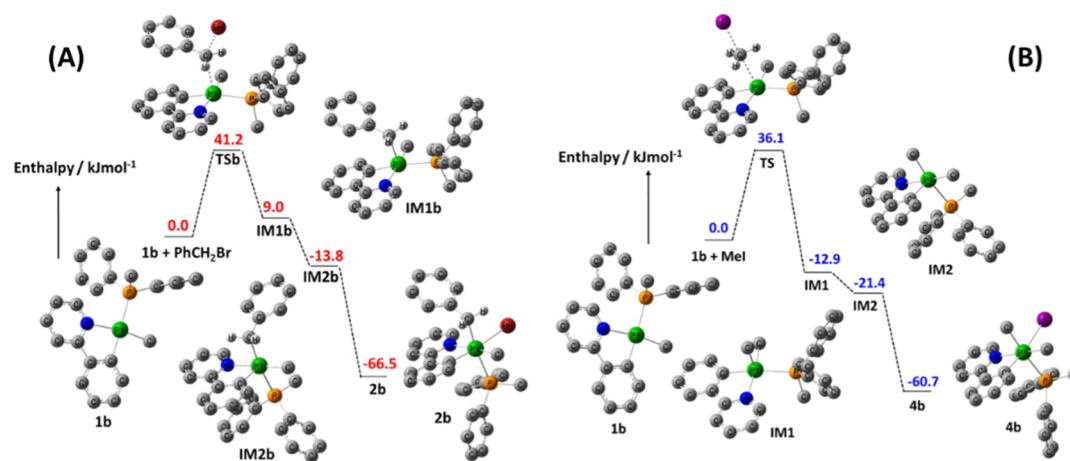


Figure 9. Enthalpy profile for oxidative addition of **1b** with (A) PhCH₂Br and (B) MeI in acetone at the B3LYP/6-31G(d)-LANL2DZ level. The optimized structures of the species involved in the reactions are shown. The summation of the energies of **1b** and PhCH₂Br or MeI was considered to be zero, and the other energy levels vary relative to this.

oxidative addition reactions of complex **1b** with PhCH₂Br and MeI in acetone are 41.2 and 36.1 kJ mol⁻¹, respectively. These observations are also consistent with the experimental values of 45.9 and 38.2 kJ mol⁻¹. As explained above, one possible interpretation for the higher energy barrier observed for PhCH₂Br *versus* MeI is that in S_N2-type reactions, the rate of reaction is dependent on the sterics of the R group: the bulkier the R group, the slower the reaction. Also, the iodide is a better leaving group than bromide.

EXPERIMENTAL SECTION

General Remarks. ¹H, ¹³C, and ³¹P NMR spectra in CDCl₃ were recorded using a Bruker Ultrashield 400 spectrometer (with TMS or 85% H₃PO₄ as references). The chemical shifts and coupling constants are in ppm and Hz, respectively. The microanalyses were performed using a ThermoFinnigan Flash EA-1112 CHNSO rapid elemental

analyzer, and melting points were recorded on a Buchi 530 apparatus. Kinetic studies were carried out using a Perkin-Elmer Lambda 25 spectrophotometer with temperature control using an EYELA NCB-3100 constant-temperature bath. Benzyl bromide and 2-(2-pyridyl)benzothiazole (abbreviated as pbt) were purchased from commercial sources, and the precursor complexes [Pt₂Me₄(μ-SMe₂)],⁸³ [PtMe₂(pbt)], **1a**,⁵⁵ [PtMe(ppy)(PPh₂Me)], **1b**,⁶⁷ [PtMe(bhq)(PPh₂Me)],**1c**,⁶⁷ and [PtMe₂(ppy)(PPh₂Me)], **4b**,⁶⁷ were prepared as reported.

Synthesis of Platinum Complexes. Preparation of [PtBr(CH₂Ph)Me₂(pbt)], **2a** + **2a'** + **2a''**. Benzyl bromide (0.014 mL, 0.12 mmol) was added to a solution of [PtMe₂(pbt)], **1a**, (0.05 g, 0.11 mmol) in dichloromethane, and the mixture was stirred at room temperature for 2 h. The solvent was evaporated from the solution, and the residue was washed with ether and *n*-hexane. The product as a light green solid was dried under vacuum. Yield: 0.063 g; 91%, mp 204 °C

(decomp.). Anal. Calcd for $C_{21}H_{21}BrN_2S$ Pt: C, 41.4; H, 3.5; N, 4.6; S, 5.3. Found: C, 41.5; H, 3.1; N, 4.7; S, 5.6. NMR data in $CDCl_3$; 1H NMR data: **2a** (major isomer): δ 1.78 [s, $^2J(PtH) = 76.0$ Hz, 3H, Me trans to N of 2-pyridyl ring], 2.05 [s, $^2J(PtH) = 76.1$ Hz, 3H, Me trans to N of benzothiazole ring], 2.90 [d, $^2J(PtH^a) = 85.0$ Hz, $^2J(H^aH^b) = 9.6$ Hz, 1H, H of CH_2Ph]; 3.11 [d, $^2J(PtH^b) = 96.3$ Hz, $^2J(H^aH^b) = 9.6$ Hz, 1H, H of CH_2Ph]; 6.29–8.65 [m, H of aromatic region], 8.68 [d, $^3J(PtH) = 12.0$ Hz, $^3J(HH) = 5.6$ Hz, 1H, CH group adjacent to coordinated 2-pyridyl N atom]. ^{13}C NMR: δ -6.4 [s, $^1J(PtC) = 680$ Hz, Me trans to N of 2-pyridyl ring], -0.2 [s, $^1J(PtC) = 712$ Hz, Me trans to N of benzothiazole ring], 22.8 [s, $^1J(PtC) = 639$ Hz, $PtCH_2$ of benzyl], 120–170 [m, C of 2-(2-pyridyl) benzothiazole ligand]. **2a'**: 1H NMR 1.71 [s, $^2J(PtH) = 72.0$ Hz, 3H, Me trans to Br], 1.98 [s, $^2J(PtH) = 72.2$ Hz, 3H, Me trans to N of benzothiazole ring], 2.87 [d, $^2J(PtH^a) = 85.2$ Hz, $^2J(H^aH^b) = 9.4$ Hz, 1H, H of CH_2Ph], 3.10 [d, $^2J(PtH^b) = 97.3$ Hz, $^2J(H^aH^b) = 9.6$ Hz, 1H, H of CH_2Ph], 8.66 [d, $^3J(PtH) =$ not resolved, $^3J(HH) = 5.6$ Hz, 1H, CH group adjacent to coordinated 2-pyridyl N atom]. ^{13}C NMR: δ -5.8 [s, $^1J(PtC) = 718$ Hz, $PtMe$]; -0.2 [s, $^1J(PtC) =$ not resolved, $PtMe$], 18.6 [s, $^1J(PtC) = 648$ Hz, $PtCH_2$ of benzyl]. ^{13}C dept NMR: δ 18.6 [s, $^1J(PtC) = 654$, $PtCH_2$ of benzyl]. 1H NMR data for **2a''**: 1.65 [s, $^2J(PtH) = 72.4$ Hz, 3H, Me trans to N of benzothiazole ring], 1.93 [s, $^2J(PtH) = 74.0$ Hz, 3H, Me trans to Br].

Preparation of [PtMeBr(CH_2Ph)(ppy)(PPh₂Me)], **2b.** This compound as a white solid was made similarly using benzyl bromide (0.014 mL, 0.12 mmol) and [PtMe(ppy)(PPh₂Me)], **1b**, (0.05 g, 0.09 mmol) for 24 h. Yield: 77%. mp 226 °C (decomp.). Anal. Calcd for $C_{32}H_{31}BrNPt$: C, 52.2; H, 4.2; N, 1.9; Found: C, 51.8; H, 3.8; N, 2.2. 1H NMR data in $CDCl_3$: δ 1.36 [d, $^3J(PH) = 7.9$ Hz, $^2J(PtH) = 68.1$ Hz, 3H, $Pt-Me$], 1.81 [d, $^2J(PH) = 9.1$ Hz, $^3J(PtH) = 11.6$ Hz, 3H, Me of PPh₂Me], 2.77 [dd, $^3J(PH) = 8.3$ Hz, $^2J(H^aH^b) = 12.8$ Hz, $^2J(PtH^a) = 49.8$ Hz, 1H, H of CH_2Ph], 3.88 [dd, $^3J(PH) = 8.3$ Hz, $^2J(H^aH^b) = 12.8$ Hz, $^2J(PtH^b) = 102.5$ Hz, 1H, H of CH_2Ph]. ^{31}P NMR: δ -18.5 [s, $^1J(PtP) = 1063$ Hz]. ^{13}C NMR: δ -3.4 [d, $^2J(PC) = 4$ Hz, $^1J(PtC) = 645$ Hz, Me trans to N of 2-pyridyl ring], 11.2 [d, $^1J(PC) = 29$ Hz, $^2J(PtC) = 16$ Hz, Me of PPh₂Me], 31.6 [d, $^2J(PC) = 106$ Hz, $^1J(PtC) = 447$ Hz, CH_2 of benzyl].

Preparation of [PtMeBr(CH_2Ph)(bhq)(PPh₂Me)], **2c.** This compound as a white solid was made similarly using benzyl bromide (0.014 mL, 0.12 mmol) and [PtMe(bhq)(PPh₂Me)] (0.04 g, 0.08 mmol) for 24 h. Yield: 62%. mp 237 °C (decomp.). Anal. Calcd for $C_{34}H_{31}BrNPt$: C, 53.7; H, 4.1; N, 1.8; Found: C, 53.5; H, 4.1; N, 2.1. 1H NMR data in $CDCl_3$: δ 1.59 (d, $^2J(PtH) = 68.6$ Hz, $^3J(PH) = 7.7$ Hz, 3H, Me group), 1.70 (d, $^3J(PtH) = 11.8$ Hz, $^2J(PH) = 9.2$ Hz, Me group of the PPh₂Me ligand), 2.74 (dd, $^3J(PH) = 9.3$ Hz, $^2J(H^aH^b) = 13.6$ Hz, $^2J(PtH^a) = 51.4$ Hz, 1H, H of CH_2Ph group), 3.92 (dd, $^3J(PH) = 9.3$ Hz, $^2J(H^aH^b) = 13.6$ Hz, $^2J(PtH^a) = 101.2$ Hz, 1H, H of CH_2Ph group), aromatic protons: 8.93 (d, $^3J(PtH) = 10.7$ Hz, $^3J(HH) = 4.2$, 1H, H¹), 7.82 (d, $^3J(HH) = 7.8$ Hz, 1H, H²), 7.66 (t, $^3J(HH) = 16.7$ Hz, 2H, H³ and H⁶), 7.51 (d, $^3J(HH) = 3.8$, 2H, H⁴ and H⁵), 7.37 (d, $^3J(HH) = 8.72$, 1H, H⁷), 7.09 (m, 4H, meta H of phenyl group of the PPh₂Me ligands), 6.97 (d, $^3J(HH) = 6.2$, 4H, ortho H of phenyl group of the PPh₂Me ligands), 6.83 (t, $^3J(HH) = 17.2$, 2H, para H of phenyl group of the PPh₂Me

ligands), 6.03–6.25 (5H, H of phenyl group of the Ph of benzyl ligand); ^{31}P NMR: δ -18.0 [s, $^1J(PtP) = 1064$ Hz].

Preparation of [Pt(Br)₂Me₂(pbt)], **4a.** To a solution of [PtMe₂(pbt)] (0.03 g, 0.069 mmol) in toluene was added an excess of benzyl bromide (0.207 mmol, 25 μ L). The reaction was refluxed at 70 °C for 6 days. The solvent was evaporated, and the residue was washed with cold diethyl ether. Yield: 77%. mp 290 °C (decomp.). Anal. Calcd for $C_{14}H_{14}Br_2N_2S$ Pt: C, 28.2; H, 2.4; N, 4.7. Found: C, 27.9; H, 2.2; N, 4.9. 1H NMR data in $CDCl_3$: δ 2.35 (s, $^2J(PtH) = 75.0$ Hz, 3H, Me), 2.61 (s, $^2J(PtH) = 75.0$ Hz, 3H, Me), aromatic protons: 8.97 (d, $^3J(PtH) = 13.1$ Hz, $^3J(HH) = 6.6$, 1H), 8.52 (d, $^3J(HH) = 7.2$ Hz, 1H), 8.20 (m, $^3J(HH) = 17.0$ Hz, 2H), 7.60–7.77 (m, 4H).

Kinetic Studies of the Oxidative Addition Reactions.

In a typical experiment, a solution of the Pt(II) complex in a cuvette was thermostated at 25 °C in acetone, and a known concentration of $PhCH_2Br$ was added using a microsyringe. After rapid stirring, the absorbance at the corresponding wavelength was collected with time. The Abs–time curves were analyzed by pseudo-first-order methods ($[PhCH_2Br]_0 \gg [1b]$ or $[1c]$) or under second-order 1:1 stoichiometric conditions ($[PhCH_2Br]_0 = [1a]$). Under pseudo-first-order conditions, the pseudo-first-order rate constants (k_{obs}) were evaluated by nonlinear least-squares fitting of the absorbance–time profiles to a first-order equation (eq 1). Then, the slope of the linear plot of k_{obs} versus $[PhCH_2Br]$ gave the second-order rate constant (k_2). In the case of second-order 1:1 stoichiometric conditions, the Abs–time data fit to eq 2 to give k_2 values.

$$Abs_t = Abs_{\infty} + (Abs_0 - Abs_{\infty}) \exp(-k_{obs}t) \quad (1)$$

$$Abs_t = Abs_{\infty} + (Abs_0 - Abs_{\infty}) / (1 + [Pt(II) \text{ complex}]_0 \times k_2 \times t) \quad (2)$$

The same method was used at other temperatures, and activation parameters were obtained from the Eyring equation (eq 3).

$$\ln\left(\frac{k_2}{T}\right) = \ln\left(\frac{k_B}{h}\right) + \frac{\Delta S^{\ddagger}}{R} - \frac{\Delta H^{\ddagger}}{RT} \quad (3)$$

Computational Details. Gaussian 09 was used⁸⁴ to fully optimize the compounds using the B3LYP level of DFT. The starting structures were created by the GaussView program and optimized using the CPCM solvation method⁸⁵ considering acetone and toluene as solvents, as implemented in the Gaussian program. The effective core potential of Hay and Wadt with a double- ξ valence basis set (LANL2DZ) was chosen to describe Pt and Br.⁸⁶ The 6-31G(d) basis set was used for all other atoms.⁸⁷ Frequency calculations were carried out at the same level of theory to identify whether the calculated stationary point is a minimum (zero imaginary frequency) or a transition-state structure (one imaginary frequency). All data were calculated at standard temperature and pressure (298.15 K and 1.0 atm.). We have also checked that imaginary frequencies exhibit the expected motion.

■ ASSOCIATED CONTENT

Supporting Information

The Supporting Information is available free of charge at <https://pubs.acs.org/doi/10.1021/acsomega.0c03573>.

Characterization and crystallographic data for complex **4a**, qualitative frontier molecular orbitals for **1a**, **TSa**, and **2a**, and Cartesian coordinates for computed structures (PDF)

CCDC 2011477 contains the supplementary crystallographic data for complex **4a** (CIF)

AUTHOR INFORMATION

Corresponding Authors

S. Masoud Nabavizadeh – Professor Rashidi Laboratory of Organometallic Chemistry, Department of Chemistry, College of Sciences, Shiraz University, Shiraz 71467-13565, Iran; orcid.org/0000-0003-3976-7869; Email: nabavizadeh@shirazu.ac.ir

Mahdi M. Abu-Omar – Department of Chemistry and Biochemistry, University of California, Santa Barbara, California 93106, United States; orcid.org/0000-0002-4412-1985; Email: abumar@chem.ucsb.edu

Authors

Marzieh Bavi – Professor Rashidi Laboratory of Organometallic Chemistry, Department of Chemistry, College of Sciences, Shiraz University, Shiraz 71467-13565, Iran

Fatemeh Niroomand Hosseini – Department of Chemistry, Shiraz Branch, Islamic Azad University, Shiraz 71993-37635, Iran; orcid.org/0000-0002-5856-8104

Fatemeh Niknam – Professor Rashidi Laboratory of Organometallic Chemistry, Department of Chemistry, College of Sciences, Shiraz University, Shiraz 71467-13565, Iran

Peyman Hamidzadeh – Professor Rashidi Laboratory of Organometallic Chemistry, Department of Chemistry, College of Sciences, Shiraz University, Shiraz 71467-13565, Iran

S. Jafar Hoseini – Professor Rashidi Laboratory of Organometallic Chemistry, Department of Chemistry, College of Sciences, Shiraz University, Shiraz 71467-13565, Iran; orcid.org/0000-0003-4514-1096

Fatemeh Raof – Professor Rashidi Laboratory of Organometallic Chemistry, Department of Chemistry, College of Sciences, Shiraz University, Shiraz 71467-13565, Iran

Complete contact information is available at:

<https://pubs.acs.org/10.1021/acsomega.0c03573>

Notes

The authors declare no competing financial interest.

ACKNOWLEDGMENTS

We acknowledge support from Shiraz University, the Iran National Science Foundation (Grants no. 97012633 and 98019717), and the Department of Chemistry and Biochemistry at UCSB.

REFERENCES

- (1) Liu, P.; Liang, R.; Lu, L.; Yu, Z.; Li, F. Use of a Cyclometalated Iridium(III) Complex Containing a N[^]C[^]N-Coordinating Terdentate Ligand as a Catalyst for the α -Alkylation of Ketones and N-Alkylation of Amines with Alcohols. *J. Org. Chem.* **2017**, *82*, 1943–1950.
- (2) Boyaala, R.; Touzani, R.; Roisnel, T.; Dorcet, V.; Caytan, E.; Jacquemin, D.; Boixel, J.; Guerschais, V.; Doucet, H.; Soulé, J.-F. Catalyst-Controlled Regiodivergent C-H Arylation Site of Fluorinated 2-Arylpyridine Derivatives: Application to Luminescent Iridium(III) Complexes. *ACS Catal.* **2018**, *9*, 1320–1328.
- (3) Blons, C.; Mallet-Ladeira, S.; Amgoune, A.; Bourissou, D. (P,C) Cyclometalated Gold(III) Complexes: Highly Active Catalysts for the

Hydroarylation of Alkynes. *Angew. Chem., Int. Ed.* **2018**, *57*, 11732–11736.

(4) Ito, J.-i.; Ishihara, T.; Fukuoka, T.; Binti Mat Napi, S. R.; Kameo, H.; Nishiyama, H. Modulation of the coordination geometries of NCN and NCNC Rh complexes for ambidextrous chiral catalysts. *Chem. Commun.* **2019**, *55*, 12765–12768.

(5) Ranieri, A. M.; Burt, L. K.; Stagni, S.; Zacchini, S.; Skelton, B. W.; Ogden, M. I.; Bissember, A. C.; Massi, M. Anionic cyclometalated platinum(II) tetrazolato complexes as viable photoredox catalysts. *Organometallics* **2019**, *38*, 1108–1117.

(6) Nabavizadeh, S. M.; Niroomand Hosseini, F.; Park, C.; Wu, G.; Abu-Omar, M. M. Discovery and mechanistic investigation of Pt-catalyzed oxidative homocoupling of benzene with PhI(OAc)₂. *Dalton Trans.* **2020**, *49*, 2477–2486.

(7) Skórka, Ł.; Filapek, M.; Zur, L.; Malecki, J. G.; Pisarski, W.; Olejnik, M.; Danikiewicz, W.; Krompiec, S. Highly phosphorescent cyclometalated iridium(III) complexes for optoelectronic applications: fine tuning of the emission wavelength through ancillary ligands. *J. Phys. Chem. C* **2016**, *120*, 7284–7294.

(8) Lu, G.; Yao, J.; Chen, Z.; Ma, D.; Yang, C. Saturated red iridium(III) complexes containing a unique four-membered Ir–S–C–N backbone: mild synthesis and application in OLEDs. *J. Mater. Chem. C* **2020**, *8*, 1391.

(9) Shao, J.-Y.; Gong, Z.-L.; Zhong, Y.-W. Bridged cyclometalated diruthenium complexes for fundamental electron transfer studies and multi-stage redox switching. *Dalton Trans.* **2018**, *47*, 23–29.

(10) Aseman, M. D.; Aryamanesh, S.; Shojaeifard, Z.; Hemmateenejad, B.; Nabavizadeh, S. M. Cycloplatinated(II) Derivatives of Mercaptopurine Capable of Binding Interactions with HSA/DNA. *Inorg. Chem.* **2019**, *58*, 16154–16170.

(11) Fereidoonhezah, M.; Ramezani, Z.; Nikravesh, M.; Zangeneh, J.; Golbon Haghighi, M.; Faghil, Z.; Notash, B.; Shahsavari, H. R. Cycloplatinated(II) complexes bearing an O,S-heterocyclic ligand: search for anticancer drugs. *New J. Chem.* **2018**, *42*, 7177–7187.

(12) Zhang, P.; Sadler, P. J. Advances in the design of organometallic anticancer complexes. *J. Organomet. Chem.* **2017**, *839*, 5–14.

(13) Graf, M.; Gothe, Y.; Metzler-Nolte, N.; Czerwiec, R.; Sünkel, K. Bis-cyclometalated rhodium- and iridium-complexes with the 4,4'-dichloro-2,2'-bipyridine ligand. Evaluation of their photophysical properties and biological activity. *Inorg. Chim. Acta* **2017**, *463*, 36–43.

(14) Barzegar-Kiadehi, S. R.; Golbon Haghighi, M.; Jamshidi, M.; Notash, B. Influence of the Diphosphine Coordination Mode on the Structural and Optical Properties of Cyclometalated Platinum(II) Complexes: An Experimental and Theoretical Study on Intramolecular Pt···Pt and π ··· π Interactions. *Inorg. Chem.* **2018**, *57*, 5060–5073.

(15) Leopold, H.; Císařová, I.; Strassner, T. Phosphorescent C[^]C* Cyclometalated Thiazol-2-ylidene Iridium(III) Complexes: Synthesis, Structure, and Photophysics. *Organometallics* **2017**, *36*, 3016–3018.

(16) Rajabi, S.; Jamali, S.; Naseri, S.; Jamjah, A.; Kia, R.; Samouei, H.; Mastroilli, P.; Shahsavari, H. R.; Raithby, P. R. Pt–M (M = Au and Tl) Dative Bonds Using Bis(cyclometalated)platinum(II) Complexes. *Organometallics* **2019**, *38*, 1709–1720.

(17) Nahaei, A.; Nabavizadeh, S. M.; Hosseini, F. N.; Hoseini, S. J.; Abu-Omar, M. M. Arene C–H bond activation and methane formation by a methylplatinum(II) complex: experimental and theoretical elucidation of the mechanism. *New J. Chem.* **2019**, *43*, 8005–8014.

(18) Zucca, A.; Petretto, G. L.; Stoccoro, S.; Cinellu, M. A.; Manassero, M.; Manassero, C.; Minghetti, G. Cyclometalation of 2,2'-Bipyridine. Mono- and Dinuclear C,N Platinum(II) Derivatives. *Organometallics* **2009**, *28*, 2150–2159.

(19) Calvet, T.; Crespo, M.; Font-Bardia, M.; Gómez, K.; González, G.; Martínez, M. Kinetic-Mechanistic Insight into the Platinum-Mediated C–C Coupling of Fluorinated Arenes. *Organometallics* **2009**, *28*, 5096–5106.

(20) Jamali, S.; Nabavizadeh, S. M.; Rashidi, M. Binuclear Cyclometalated Organoplatinum Complexes Containing 1,1'-Bis-(diphenylphosphino)ferrocene as Spacer Ligand: Kinetics and

Mechanism of MeI Oxidative Addition. *Inorg. Chem.* **2008**, *47*, 5441–5452.

(21) Niknam, F.; Hamidzadeh, P.; Nabavizadeh, S. M.; Niroomand Hosseini, F.; Hoseini, S. J.; Ford, P. C.; Abu-Omar, M. M. Synthesis, structural characterization, and luminescence properties of mono- and di-nuclear platinum(II) complexes containing 2-(2-pyridyl)-benzimidazole. *Inorg. Chim. Acta* **2019**, *498*, 119133–119142.

(22) Nahaei, A.; Rasekh, A.; Rashidi, M.; Hosseini, F. N.; Nabavizadeh, S. M. Phenylpyrazolate cycloplatinated(II) complexes: Kinetics of oxidation to Pt(IV) complexes. *J. Organomet. Chem.* **2016**, *815–816*, 35–43.

(23) Aghakhanpour, R. B.; Nabavizadeh, S. M.; Rashidi, M. Newly designed luminescent di- and tetra-nuclear double rollover cycloplatinated(II) complexes. *J. Organomet. Chem.* **2016**, *819*, 216–227.

(24) Solomatina, A. I.; Chelushkin, P. S.; Krupenya, D. V.; Podkorytov, I. S.; Artamonova, T. O.; Sizov, V. V.; Melnikov, A. S.; Gurchiy, V. V.; Koshel, E. I.; Shcheslavskiy, V. I.; Tunik, S. P. Coordination to imidazole ring switches on phosphorescence of platinum cyclometalated complexes: the route to selective labeling of peptides and proteins via histidine residues. *Bioconjugate Chem.* **2017**, *28*, 426–437.

(25) Leopold, H.; Tronnier, A.; Wagenblast, G.; Münster, I.; Strassner, T. Photoluminescence of a New Material: Cyclometalated C[∧]C* Thiazole-2-ylidene Platinum(II) Complexes. *Organometallics* **2016**, *35*, 959–971.

(26) Moussa, J.; Loch, A.; Chamoreau, L.-M.; Degli Esposti, A.; Bandini, E.; Barbieri, A.; Amouri, H. Luminescent Cyclometalated Platinum Complexes with π -Bonded Catecholate Organometallic Ligands. *Inorg. Chem.* **2017**, *56*, 2050–2059.

(27) Fereidoonzehad, M.; Kaboudin, B.; Mirzaee, T.; Babadi Aghakhanpour, R.; Golbon Haghghi, M.; Faghhi, Z.; Faghhi, Z.; Ahmadipour, Z.; Notash, B.; Shahsavari, H. R. Cyclometalated Platinum(II) Complexes Bearing Bidentate O,O'-Di(alkyl)-dithiophosphate Ligands: Photoluminescence and Cytotoxic Properties. *Organometallics* **2017**, *36*, 1707–1717.

(28) Jamshidi, M.; Babaghasabha, M.; Shahsavari, H. R.; Nabavizadeh, S. M. The influence of thiolate ligands on the luminescence properties of cycloplatinated(II) complexes. *Dalton Trans.* **2017**, *46*, 15919–15927.

(29) Crespo, M.; Martínez, M.; Nabavizadeh, S. M.; Rashidi, M. Kinetic-mechanistic studies on CX (X=H, F, Cl, Br, I) bond activation reactions on organoplatinum(II) complexes. *Coord. Chem. Rev.* **2014**, *279*, 115–140.

(30) Rendina, L. M.; Puddephatt, R. J. Oxidative addition reactions of organoplatinum(II) complexes with nitrogen-donor ligands. *Chem. Rev.* **1997**, *97*, 1735–1754.

(31) Dicciani, J. B.; Katigbak, J.; Hu, C.; Diao, T. Mechanistic Characterization of (Xantphos)Ni(I)-Mediated Alkyl Bromide Activation: Oxidative Addition, Electron Transfer, or Halogen-Atom Abstraction. *J. Am. Chem. Soc.* **2019**, *141*, 1788–1796.

(32) Kehoe, R.; Mahadevan, M.; Manzoor, A.; McMurray, G.; Wienefeld, P.; Baird, M. C.; Budzelaar, P. H. M. Reactions of the Ni(0) Compound Ni(PPh₃)₄ with Unactivated Alkyl Halides: Oxidative Addition Reactions Involving Radical Processes and Nickel(I) Intermediates. *Organometallics* **2018**, *37*, 2450–2467.

(33) Hamidzadeh, P.; Nabavizadeh, S. M.; Hoseini, S. J. Effects of the number of cyclometalated rings and ancillary ligands on the rate of MeI oxidative addition to platinum(II)-pincer complexes. *Dalton Trans.* **2019**, *48*, 3422–3432.

(34) Azizpoor Fard, M.; Behnia, A.; Puddephatt, R. J. Models for Cooperative Catalysis: Oxidative Addition Reactions of Dimethylplatinum(II) Complexes with Ligands Having Both NH and OH Functionality. *ACS Omega* **2019**, *4*, 257–268.

(35) Pichaandi, K. R.; Kaban, L.; Amini, H.; Zhang, G.; Zhu, H.; Kenttämaa, H. I.; Fanwick, P. E.; Miller, J. T.; Kais, S.; Nabavizadeh, S. M.; Rashidi, M.; Abu-Omar, M. M. Mechanism of Me-Re Bond Addition to Platinum(II) and Dioxygen Activation by the Resulting Pt-Re Bimetallic Center. *Inorg. Chem.* **2017**, *56*, 2145–2152.

(36) Fard, M. A.; Behnia, A.; Puddephatt, R. J. Cycloneophylplatinum Chemistry: A New Route to Platinum(II) Complexes and the Mechanism and Selectivity of Protonolysis of Platinum-Carbon Bonds. *Organometallics* **2018**, *37*, 3368–3377.

(37) Aseman, M. D.; Rashidi, M.; Nabavizadeh, S. M.; Puddephatt, R. J. Secondary kinetic isotope effects in oxidative addition of benzyl bromide to dimethylplatinum(II) complexes. *Organometallics* **2013**, *32*, 2593–2598.

(38) Niroomand Hosseini, F.; Nabavizadeh, S. M.; Abu-Omar, M. M. Which is the Stronger Nucleophile, Platinum or Nitrogen in Rollover Cycloplatinated(II) Complexes? *Inorg. Chem.* **2017**, *56*, 14706–14713.

(39) Maidich, L.; Zucca, A.; Clarkson, G. J.; Rourke, J. P. Oxidative Addition of MeI to a Rollover Complex of Platinum(II): Isolation of the Kinetic Product. *Organometallics* **2013**, *32*, 3371–3375.

(40) Whitfield, S. R.; Sanford, M. S. Reactions of platinum(II) complexes with chloride-based oxidants: routes to Pt(III) and Pt(IV) products. *Organometallics* **2008**, *27*, 1683–1689.

(41) Hartwig, J. F. *Organotransition Metal Chemistry: From Bonding to Catalysis*; Univ Science Books, 2010.

(42) Grubbs, R. H. *Organometallic Chemistry in Industry: A Practical Approach*; John Wiley & Sons, 2020.

(43) Albrecht, M.; Gossage, R. A.; Spek, A. L.; van Koten, G. Metal-Mediated C–C Bond Making and Breaking: First Direct Evidence for a Reversible Migration of a Benzyl Group along a Metal–Carbon Bond. *J. Am. Chem. Soc.* **1999**, *121*, 11898–11899.

(44) McCreedy, M. S.; Puddephatt, R. J. Supramolecular Organoplatinum(IV) Chemistry: Dimers and Polymers Formed by Intermolecular Hydrogen Bonding. *ACS Omega* **2018**, *3*, 13621–13629.

(45) Aseman, M. D.; Nabavizadeh, S. M.; Niroomand Hosseini, F.; Wu, G.; Abu-Omar, M. M. Carbon-Oxygen Bond Forming Reductive Elimination from Cycloplatinated(IV) Complexes. *Organometallics* **2018**, *37*, 87–98.

(46) Anderson, C. M.; Brown, G.; Greenberg, M. W.; Yu, D.; Bowen, N.; Ahmed, R.; Yost-Bido, M.; Wray, A. Stereoselective CX and regioselective CH activation to, and selective C(sp²)-C(sp³) reductive elimination from, platinum compounds with thiophene-derived ligands. *Tetrahedron Lett.* **2019**, *60*, 151156.

(47) Sarju, J. P.; Dey, D.; Torroba, J.; Whitwood, A. C.; Redeker, K.; Bruce, D. W. Catalytic Activation of Unstrained, Nonactivated Ketones Mediated by Platinum(II): Multiple C-C Bond Cleavage and CO Extrusion. *Organometallics* **2019**, *38*, 4539–4542.

(48) Shiba, Y.; Inagaki, A.; Akita, M. C-C Bond Forming Reductive Elimination from Diarylplatinum Complexes Driven by Visible-Light-Mediated Photoredox Reactions. *Organometallics* **2015**, *34*, 4844–4853.

(49) Liberman-Martin, A. L.; Bergman, R. G.; Tilley, T. D. A remote Lewis acid trigger dramatically accelerates biaryl reductive elimination from a platinum complex. *J. Am. Chem. Soc.* **2013**, *135*, 9612–9615.

(50) Brown, M. P.; Puddephatt, R. J.; Upton, C. E. E.; Lavington, S. W. Thermal decomposition of some acyl(dialkyl)-, dialkyl(allyl)-, dialkyl(benzyl)-, and trialkyl-halogenobis(dimethylphenylphosphine)-platinum(IV) complexes. *J. Chem. Soc., Dalton Trans.* **1974**, 1613–1618.

(51) Shahsavari, H. R.; Babadi Aghakhanpour, R.; Biglari, A.; Niazi, M.; Mastrorilli, P.; Todisco, S.; Gallo, V.; Lalinde, E.; Moreno, M. T.; Giménez, N.; Halvagar, M. R. C(sp²)-C(sp²) Reductive Elimination from a Diarylplatinum(II) Complex Induced by a S–S Bond Oxidative Addition at Room Temperature. *Organometallics* **2020**, *39*, 417–424.

(52) Zanganeh, M.; Hoseini, S. J.; Rashidi, M.; Nabavizadeh, S. M.; Halvagar, M. R. Reaction of allyl bromide with cyclometalated platinum(II) complexes: Unusual kinetic behavior and a novel case of methyl and allyl C-C bond reductive elimination. *J. Organomet. Chem.* **2018**, *856*, 1–12.

(53) van Asselt, R.; Rijnberg, E.; Elsevier, C. J. Rigid bidentate nitrogen ligands in organometallic chemistry and homogeneous catalysis. 7. Stabilization of high oxidation states by rigid bidentate

nitrogen ligands: synthesis and characterization of diorgano- and triorganopalladium(IV) and cationic triorganoplatinum(IV) complexes. *Organometallics* **1994**, *13*, 706–720.

(54) Crumpton, D. M.; Goldberg, K. I. Five-Coordinate Intermediates in Carbon–Carbon Reductive Elimination Reactions from Pt(IV). *J. Am. Chem. Soc.* **2000**, *122*, 962–963.

(55) Nabavizadeh, S. M.; Raof, F.; Pakpour, F.; Shafiei Sarvestani, L.; Niknam, F.; Niroomand Hosseini, F.; Hoseini, S. J. Facile activation of the C–I bond of primary alkyl halides by Pt(II) complexes having a benzothiazole ligand. *Inorg. Chim. Acta* **2020**, *506*, 119535–119543.

(56) Fard, M. A.; Behnia, A.; Puddephatt, R. J. Supramolecular Polymer and Sheet and a Double Cubane Structure in Platinum(IV) Iodide Chemistry: Solution of a Longstanding Puzzle. *ACS Omega* **2018**, *3*, 10267–10272.

(57) Suzuki, Y.; Kihō, M.; Osakada, K. Fluoroalkylation of a Methylplatinum(II) Complex under Photoirradiation. *Organometallics* **2017**, *36*, 1391–1397.

(58) Azizpoor Fard, M.; Behnia, A.; Puddephatt, R. J. Activation of Dioxxygen by Dimethylplatinum(II) Complexes. *Organometallics* **2017**, *36*, 4169–4178.

(59) Niazi, M.; Shahsavari, H. R. Cycloplatinated(II) complex bearing 2-vinylpyridine and monodentate phosphine ligands: Optical properties and kinetic study. *J. Organomet. Chem.* **2016**, *803*, 82–91.

(60) Thompson, K. A.; Kadwell, C.; Boyle, P. D.; Puddephatt, R. J. Reactivity of organoplatinum complexes containing appended alcohol functional groups: Activation of dioxxygen and hydrogen peroxide. *J. Organomet. Chem.* **2017**, *829*, 22–30.

(61) Shahsavari, H. R.; Rashidi, M.; Nabavizadeh, S. M.; Habibzadeh, S.; Heinemann, F. W. A Tetramethylplatinum(IV) Complex with 1,1'-Bis(diphenylphosphanyl)ferrocene Ligands: Reaction with Trifluoroacetic Acid. *Eur. J. Inorg. Chem.* **2009**, 3814–3820.

(62) Brown, M. P.; Puddephatt, R. J.; Upton, C. E. E. Mechanism of reductive elimination of ethane from some halogenotrimethylbis(tertiary phosphine)platinum(IV) complexes. *J. Chem. Soc., Dalton Trans.* **1974**, 2457–2465.

(63) Momeni, B. Z.; Hadi, S.; Biglari, A. Design of alkyl- and haloalkyl complexes of dimethylplatinum(IV) via oxidative addition: Reactivity, characterization and crystal structures. *Inorg. Chim. Acta* **2017**, *455*, 262–270.

(64) Momeni, B. Z.; Rashidi, M.; Jafari, M. M.; Patrick, B. O.; Abd-El-Aziz, A. S. Oxidative addition of some mono, di or tetra haloalkanes to organoplatinum(II) complexes. *J. Organomet. Chem.* **2012**, *700*, 83–92.

(65) Hoseini, S. J.; Nasrabadi, H.; Nabavizadeh, S. M.; Rashidi, M.; Puddephatt, R. J. Reactivity and Mechanism in the Oxidative Addition of Allylic Halides to a Dimethylplatinum(II) Complex. *Organometallics* **2012**, *31*, 2357–2366.

(66) Hadadi, E.; Nabavizadeh, S. M.; Niroomand Hosseini, F. Platinum-oxygen Bond Formation: Kinetic and Mechanistic Studies. *Inorg. Chem. Res.* **2019**, *2*, 117–128.

(67) Nabavizadeh, S. M.; Amini, H.; Jame, F.; Khosraviolya, S.; Shahsavari, H. R.; Niroomand Hosseini, F.; Rashidi, M. Oxidative addition of MeI to some cyclometalated organoplatinum(II) complexes: Kinetics and mechanism. *J. Organomet. Chem.* **2012**, *698*, 53–61.

(68) Nabavizadeh, S. M.; Hoseini, S. J.; Momeni, B. Z.; Shahabadi, N.; Rashidi, M.; Pakiari, A. H.; Eskandari, K. Oxidative addition of n-alkyl halides to diimine-dialkylplatinum(II) complexes: a closer look at the kinetic behaviors. *Dalton Trans.* **2008**, 2414–2421.

(69) Sangari, M. S.; Rashidi, M.; Nabavizadeh, S. M.; Askari, B.; Niroomand Hosseini, F. Reaction of dimethylplatinum(II) complexes with PhCH₂CH₂Br: Comparative reactivity with CH₃CH₂Br and PhCH₂Br and synthesis of Pt(IV) complexes. *Appl. Organomet. Chem.* **2018**, *32*, e3954.

(70) Rashidi, M.; Nabavizadeh, M.; Hakimelahi, R.; Jamali, S. Kinetics and mechanism of cleavage of the oxygen-oxygen bond in

hydrogen peroxide and dibenzoyl peroxide by arylplatinum(II) complexes. *J. Chem. Soc., Dalton Trans.* **2001**, 3430–3434.

(71) Cramer, C. J.; Truhlar, D. G. Density functional theory for transition metals and transition metal chemistry. *Phys. Chem. Chem. Phys.* **2009**, *11*, 10757–10816.

(72) Lin, Z. Interplay between theory and experiment: computational organometallic and transition metal chemistry. *Acc. Chem. Res.* **2010**, *43*, 602–611.

(73) Bencini, A. Some considerations on the proper use of computational tools in transition metal chemistry. *Inorg. Chim. Acta* **2008**, *361*, 3820–3831.

(74) Ghari, H.; Li, Y.; Roohzadeh, R.; Caramenti, P.; Waser, J.; Ariafard, A. Gold-catalyzed domino cyclization-alkynylation reactions with EBX reagents: new insights into the reaction mechanism. *Dalton Trans.* **2017**, *46*, 12257–12262.

(75) Chipman, A.; Yates, B. F.; Canty, A. J.; Ariafard, A. Reduction of a platinum(IV) prodrug model by sulfur containing biological reductants: computational mechanistic elucidation. *Chem. Commun.* **2018**, *54*, 10491–10494.

(76) Fiuzza, S. M.; Amado, A. M.; Marques, M. P. M.; Batista de Carvalho, L. A. E. Use of Effective Core Potential Calculations for the Conformational and Vibrational Study of Platinum(II) Anticancer Drugs. cis-Diamminedichloroplatinum(II) as a Case Study. *J. Phys. Chem. A* **2008**, *112*, 3253–3259.

(77) Nabavizadeh, S. M.; Niroomand Hosseini, F.; Nejabat, N.; Parsa, Z. Bismuth-Halide Oxidative Addition and Bismuth-Carbon Reductive Elimination in Platinum Complexes Containing Chelating Diphosphine Ligands. *Inorg. Chem.* **2013**, *52*, 13480–13489.

(78) Hosseini, F. N.; Ariafard, A.; Rashidi, M.; Azimi, G.; Nabavizadeh, S. M. Density functional studies of influences of Ni triad metals and solvents on oxidative addition of MeI to [M(CH₃)₂(NH₃)₂] complexes and C–C reductive elimination from [M(CH₃)₃(NH₃)₂I] complexes. *J. Organomet. Chem.* **2011**, *696*, 3351–3358.

(79) Safa, M.; Jennings, M. C.; Puddephatt, R. J. Reactivity of a Dimethylplatinum(II) Complex with the Bis(2-pyridyl)dimethylsilane Ligand: Easy Silicon-Carbon Bond Activation. *Organometallics* **2012**, *31*, 3539–3550.

(80) Gilbert, T. M.; Hristov, I.; Ziegler, T. Comparison between Oxidative Addition and σ -Bond Metathesis as Possible Mechanisms for the Catalytic Methane Activation Process by Platinum(II) Complexes: A Density Functional Theory Study. *Organometallics* **2001**, *20*, 1183–1189.

(81) Zeng, G.; Sakaki, S. Noble Reaction Features of Bromoborane in Oxidative Addition of B–Br σ -Bond to [M(PMe₃)₂] (M = Pt or Pd): Theoretical Study. *Inorg. Chem.* **2011**, *50*, 5290–5297.

(82) Ateşin, T. A.; Jones, W. D. A Deeper Look into Thiophene Coordination Prior to Oxidative Addition of the C–S Bond to Platinum(0): A Computational Study Using DFT and MO Methods. *Organometallics* **2008**, *27*, 53–60.

(83) Scott, J. D.; Puddephatt, R. J. Ligand dissociation as a preliminary step in methyl-for-halogen exchange reactions of platinum(II) complexes. *Organometallics* **1983**, *2*, 1643–1648.

(84) Frisch, M.; Trucks, G.; Schlegel, H. B.; Scuseria, G.; Robb, M.; Cheeseman, J.; Scalmani, G.; Barone, V.; Mennucci, B.; Petersson, G. *Gaussian 09*, revision D. 01; Gaussian, Inc.: Wallingford CT, 2009.

(85) Cossi, M.; Rega, N.; Scalmani, G.; Barone, V. Energies, structures, and electronic properties of molecules in solution with the C-PCM solvation model. *J. Comput. Chem.* **2003**, *24*, 669–681.

(86) Hay, P. J.; Wadt, W. R. Ab initio effective core potentials for molecular calculations. Potentials for the transition metal atoms Sc to Hg. *J. Chem. Phys.* **1985**, *82*, 270–283.

(87) Hariharan, P. C.; Pople, J. A. The influence of polarization functions on molecular orbital hydrogenation energies. *Theor. Chim. Acta* **1973**, *28*, 213–222.